Biochemical Pharmacology, Vol. 44, No. 4, pp. 651–658, 1992.
Printed in Great Britain.

0006-2952/92 $5.00 + 0.00

THE MICROSOMAL DEMETHYLATION OF *N,N*-DIMETHYLBENZAMIDES

SUBSTITUENT AND KINETIC DEUTERIUM ISOTOPE EFFECTS

LUIS CONSTANTINO, EDUARDA ROSA and JIM ILEY*†

CECF, Faculdade de Farmácia de Lisboa, Avenida das Forças Armadas, 1600 Lisboa, Portugal; and *Physical Organic Chemistry Research Group, Chemistry Department, The Open University, Milton Keynes MK7 6AA, U.K.

(*Received* 1 *May* 1992; *accepted* 4 *June* 1992)

Abstract—The metabolism of *N,N*-dimethylbenzamides by phenobarbital-induced rat liver microsomes results in the formation of *N*-methylbenzamides and formaldehyde. The reaction proceeds via the formation of an intermediate *N*-hydroxymethyl-*N*-methylbenzamide, which, for the microsomal oxidation of *N,N*-dimethylbenzamide, was isolated and characterized. Confirmation of the *N*-hydroxymethyl-*N*-methylbenzamide was obtained by its independent synthesis from *N*-methylbenzamide and formaldehyde. The intermolecular kinetic deuterium isotope effects for the reaction are 0.9 (±0.1) for V_{max} and 1.4 (±0.1) for V_{max}/K_m. The intramolecular kinetic deuterium isotope effect, determined from the relative amounts of *N*-methylbenzamide and *N*-trideuteriomethylbenzamide formed in the microsomal demethylation of *N*-trideuteriomethyl-*N*-methylbenzamide, is 6.0 ± 0.3. There is no correlation of V_{max} or V_{max}/K_m with the substituent in the aromatic ring, nor with the calculated ionization potentials of the benzamides. The results are interpreted in terms of a mechanism in which the benzamide undergoes direct hydrogen atom abstraction to form a carbon centred radical. This carbon centred radical subsequently forms an *N*-hydroxymethyl-*N*-methylbenzamide that decomposes to formaldehyde and an *N*-methylbenzamide. Semi-empirical AM1 self consistent field molecular orbital calculations identify that loss of a hydrogen atom from the *E*-methyl group is thermodynamically more favourable than from the *Z*-methyl group by *ca.* 5 kJ/mol.

The cytochrome P450 enzymes are a series of structurally related isoenzymes that play a strategic role in many biotransformations of organic compounds, either of those found in the organism (endogenous) or those ingested environmentally or administered as drugs (xenobiotic). The enzymes function as monooxygenases, utilizing an oxygen atom from a dioxygen molecule, often resulting in the insertion of one atom of oxygen into an organic substrate [1]. For example, alkanes are metabolized to alcohols, aromatic compounds to phenols, alkenes to epoxides, sulphur compounds to sulphoxides and sulphones, and alicyclic compounds can be aromatized [2]. Alternatively, cytochrome P450 enzymes can bring about bond cleavage reactions, especially of the bonds between carbon and heteroatoms, e.g. nitrogen, oxygen [3]. These often proceed by way of an oxygen insertion reaction to form an unstable intermediate that decomposes by cleavage of the C—X bond:

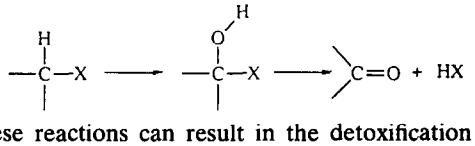

These reactions can result in the detoxification of the substrate (by making it more hydrophilic and more readily excreted) or in substrate activation. A great many of the xenobiotic compounds that are exposed to P450 metabolism are based on the dialkylamino functionality, R^1R^2N–, whether as tertiary amines (e.g. nicotine, 1-(1-phenycyclohexyl)piperidines, the tricyclic antidepressants), dialkylamides (e.g. the benzodiazepine anxiolytics, industrial solvents such as *N,N*-dimethylformamide, insect repellents such as *N,N*-diethyl-*m*-toluamide, barbiturates) or other related groups such as dialkylnitrosamines (environmental carcinogens) and dialkyltriazenes (anticancer agents). As a consequence, the study of such reactions is important to the understanding of the pharmacology and toxicology of these compounds.

Recently, we used substituent and kinetic deuterium isotope effects to identify the pathway for the microsomal metabolism of *N,N*-dimethyltriazines [4]. We have now turned our attention to the use of these techniques to investigate the molecular pathway by which the corresponding amides are metabolized. In part, this is because amides are less electron rich than triazenes (for example, the ionization potential of *N,N*-dimethylbenzamide is 9.55 eV whereas that for 1-phenyl-3,3-dimethyltriazine is 8.71 eV) and, in part, because a variety of *N,N*-dialkylamides have important biological activity. For example, *N,N*-diethylnicotinamide (nikethamide) is a respiratory stimulant [5] and *N,N*-diethyl-3-toluamide is the most commonly used insect repellent world wide [6]. *N,N*-Dimethylformamide is an industrially important

† Corresponding author: Dr J. Iley, Chemistry Department, The Open University, Milton Keynes MK7 6AA, U.K. Tel. (0908) 652513; FAX (0908) 653744.

solvent that is a suspected carcinogen and some *N*-alkyl and *N,N*-dialkylamides show activity against certain forms of cancer [7]. All these compounds are known to undergo oxidative N-dealkylation by *in vivo* metabolism by the liver.

Our initial studies involved the biomimetic oxidative demethylation reactions of model compounds, namely *N,N*-dimethylbenzamides, using a tetraphenylporphyrinatoiron (III) chloride/*t*-butylhydroperoxide system. The reaction proceeds with formation of *N*-formyl-*N*-methylbenzamide and the substituent and kinetic deuterium isotope effects suggest a mechanism involving a direct hydrogen atom abstraction [8]. In this paper we present analogous results for the N-demethylation reaction using rat liver microsomes, which enable us to propose a mechanism for the microsomal oxidation of *N,N*-dimethylamides.

The compounds employed for the present studies are **1**; **a–f**:

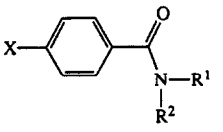

1

	X	R^1	R^2
(a)	H	CH_3	CH_3
(b)	H	CD_3	CD_3
(c)	H	CH_3	CD_3
(d)	MeO	CH_3	CH_3
(e)	Cl	CH_3	CH_3
(f)	O_2N	CH_3	CH_3

MATERIALS AND METHODS

Substrates. The *N,N*-dimethylbenzamides, **1**; **a**, **b**, **d–f**, and their *N*-methyl analogues were synthesized by the Schotten–Baumann method from the appropriate benzoyl chloride and parent amine [9]. The compounds were purified by column chromatography using ethyl acetate–hexane (5:2) as eluant. *N*-Methyl-*N*-trideuteriomethylbenzamide, **1c**, was synthesized from *N*-methylbenzamide (**3**; Ar = Ph) as follows. The monomethylbenzamide (1 g) was dissolved in dry tetrahydrofuran (30 cm^3) under N_2 at room temperature and *n*-butyllithium (1.1 mol equivalents) was injected slowly into the solution. After 15 min, a solution of iodotrideuteriomethane (1.2 mol equivalents) in 10 cm^3 of dry tetrahydrofuran was added and the solution stirred for 45 min. Ethanol (5 cm^3) was then added, the solvents evaporated, and the residue was dissolved in ethyl acetate (30 cm^3), washed with water (2 × 10 cm^3), dried ($MgSO_4$), concentrated and subjected to chromatography on silica using ethyl acetate as eluant. The product was further purified by semi-preparative HPLC using a C-18 column and acetonitrile–water (20:80) as eluant. The product, which was an oil, had δ_H/ppm (D_2O): 3.05 (3H, s) and 7.42–7.48 (5H,m), and *m/z* 152, 151, 105 and 77. The intensity of the *m/z* 151 and 148 peaks, 62% and 0.2%, respectively, indicated that the compound had >99.66% incorporation of a trideuteriomethyl group.

N-Hydroxymethyl-*N*-methylbenzamide (**2**; Ar = Ph) was synthesized by dissolving *N*-methylbenzamide (1.5 g) in aqueous formaldehyde solution (25 cm^3, 37% w/v) at neutral pH. The reaction was followed by HPLC using a C18 column and acetonitrile–water (20:80) as eluant. After 18 hr the solution was concentrated and *N*-hydroxymethyl-*N*-methylbenzamide was separated from *N*-methylbenzamide by semi-preparative HPLC using a C18 column and acetonitrile–water (10:90) as eluant. A yield of 11% was obtained; all attempts to increase the yield by employing longer reaction times, a pH of 3 or carrying out the reaction in different solvents, e.g. ethanol, were unsuccessful. The product was a solid, m.p. 95–97°, and had δ_H/ppm (dimethyl sulphoxide) 2.99 (3H, s), 4.64 (2H, s), 6.14 (1H, s exch.), 7.46 (5H, s); δ_{13C}/ppm (D_2O) (*E* and *Z* isomers) 34.8, 38.9 (CH_3), 76.8, 72.9 (CH_2), 129.3, 129.4, 131.4, 133.3 (aromatic), 177.5 (C=O); *m/z* (%) = 165 (1) ($M^{+\cdot}$), 134 (14) (M—CH_2OH), 105 (44) ($PhCO^+$), 77 (42) (Ph^+), 18 (100) ($H_2O^{+\cdot}$); ν_{max}/cm^{-1} (KBr): 3352, 1611, 1407, 1277, 1261, 1042, 1019.

Microsomes. Ten-week-old male Wistar rats were injected intraperitoneally with 80 mg/kg/day of phenobarbital for 4 days, starved for 1 day and killed by decapitation 24 hr after the last injection. The livers were removed, immersed in ice-cold 50 mmol/dm^3 Tris–HCl buffer containing 154 mmol/dm^3 KCl, minced, washed and then homogenized in a teflon/glass homogenizer immersed in ice using 3 cm^3 of washing solution/g of liver. The homogenate was first centrifuged at 10,000 *g* for 20 min at 4°. The pellet was discarded and the supernatant was centrifuged again at 100,000 *g* for 1 hr at 4°. The 100,000 *g* supernatant was discarded and the pellet resuspended in phosphate buffer (68 mmol/dm^3, pH 7.4 containing 74 mmol/dm^3 NaCl) (PBS) and stored at −80°.

The protein concentration was determined by the method of Lowry *et al.* [10]. Cytochrome P450 analysis was performed by determining the difference in absorbance at 450 and 490 nm after passing carbon monoxide through a suspension of the microsomes treated with sodium dithionite [11]. Cytochrome P450 levels were 1.5 nmol/mg protein.

Products. The reactions were quenched by the sequential addition of 0.20 mol/dm^3 $ZnSO_4$ and 0.16 mol/dm^3 $BaCl_2$. After centrifugation, the supernatant was analysed for formaldehyde by the Nash procedure [12] or for the amides by HPLC.

HPLC analysis. Separation of the amides was achieved using a 5 μm RP-18 25 cm (Merck) column and an eluant consisting of a 20:80 mixture of acetonitrile–water for **1**; **a–c**; a 25:75 mixture of acetonitrile–water for **1d**; a 30:70 mixture of acetonitrile–water for **1e** and a 27.5:72.5 mixture of acetonitrile–water for **1f**. The wavelength used for detection was 254 nm. Separate injections were reproducible to ±1.5%, and concentrations of amides measured by this technique were accurate to ±2%.

Reaction kinetics. Incubations were performed in pH 7.4 PBS using 3.1 mg protein/cm^3 of microsomes,

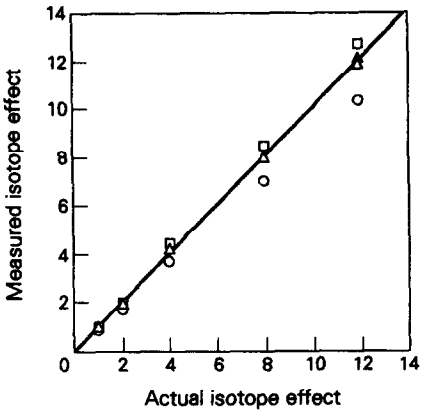

Fig. 1. Mass spectral calibration curve for mixtures of *N*-methyl- and *N*-trideuteriomethyl-benzamides. (□) m/z = 138:135 uncorrected; (△) m/z = 138:135 corrected; (○) m/z = 137: 134 uncorrected; (▲) m/z = 137:134 corrected.

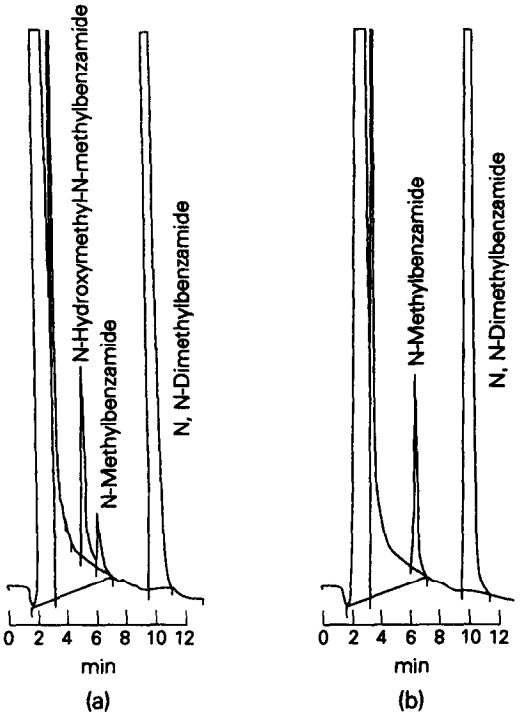

Fig. 2. HPLC traces of the incubation mixture of **1a** prior to (a) and following (b) treatment with NaOH.

6.25 mmol/dm^3 glucose-6-phosphate, 1.25 mmol/dm^3 NADP, 6 mmol/dm^3 $MgCl_2$ and 2.5 U/cm^3 of glucose-6-phosphate dehydrogenase. Reactions were started by the addition of the substrate dissolved in pH 7.4 PBS. Substrate concentrations used were 0.5–10 mmol/dm^3. Aliquots (0.1 cm^3) were withdrawn at timed intervals and quenched by the sequential addition of 0.4 cm^3 of $ZnSO_4$ (0.2 mmol/dm^3) and 0.4 cm^3 of $BaCl_2$ (0.16 mmol/dm^3). After centrifugation, 0.75 cm^3 of the supernatant was treated with 0.2 cm^3 of NaOH (1 mol/dm^3) for 10 min and 0.25 cm^3 of HCl (1 mol/dm^3). *N*-Methylbenzamides were analysed by HPLC, and formaldehyde was analysed by the Nash procedure. Alternatively, for the *N*-hydroxymethyl-*N*-methylbenzamides the supernatant was analysed directly by HPLC. Measurement of amide concentrations following the above procedure were reproducible to ±2%.

Mass spectral assay for N-*trideuteriomethylbenzamide and* N-*methylbenzamide.* *N*-Trideuteriomethyl-*N*-methyl benzamide **1c** (10 mmol/dm^3) was subjected to microsomal oxidation as described above. The reaction was followed by HPLC and every 2 hr more glucose-6-phosphate, NADPH and glucose-6-phosphate dehydrogenase were added until 50% of the substrate was metabolized. The reaction was stopped by the addition of $ZnSO_4$ (0.2 mmol/dm^3) and $BaCl_2$ (0.16 mmol/dm^3). After centrifugation, the supernatant was saturated with ammoniun carbonate and extracted three times with ethyl acetate. The organic phase was dried (sodium sulfate), concentrated and analysed by GC–MS (BP-5 column, 25 m, start temperature 80° then 10°/min up to 200°, Hewlett–Packard 5890-A/VG Mass lab 20–250).

Isotopic composition of the *N*-trideuteriomethylbenzamide/*N*-methylbenzamide component was determined by comparison of the intensities of the two molecular ion peaks at m/z = 138 (*N*-trideuteriomethylbenzamide) and 135 (*N*-methylbenzamide) using a calibration graph obtained from gravimetrically prepared mixtures of the two benzamides. The [M-1] peaks at m/z = 137/134 peaks gave analogous results (Fig. 1). Direct comparison of the m/z = 138 and m/z = 135 peaks slightly overestimates the true isotope effect, whereas direct comparison of the m/z = 137 and m/z = 134 peaks underestimates it (Fig. 1). This is due to the relative intensities of the $M^{+\cdot}$ and $[M\text{-}1]^{+\cdot}$ ions for each of the isotopomeric compounds. For *N*-methylbenzamide, the most intense ion is m/z = 105; using this ion as 100%, the intensities of the m/z = 134 and 135 ions are 67.3% and 40.6%, respectively. Similarly, for *N*-trideuteriomethylbenzamide the most intense ion is also m/z = 105; however, the relative intensities of the m/z = 137 and 138 peaks are 58.5% and 42.5%, respectively. Correcting the calibration graphs for these differences in intensities produces the expected line of unit slope.

Isolation of N-*hydroxymethyl*-N-*methylbenzamide.* *N,N*-Dimethylbenzamide was subjected to microsomal oxidation using the conditions described above for the mass spectral assay. After 6 hr the reaction was stopped by the sequential addition of $ZnSO_4$ and $BaCl_2$. Following centrifugation, the supernatant was freeze-dried, dissolved in the minimum amount of water and separated by semi-preparative HPLC using a C18 column and acetonitrile–water (10:90) as eluant.

Molecular orbital calculations. Structural determinations and ionization potentials for the dimethylbenzamides were calculated using the semi-empirical AM1 self consistent field molecular orbital program within the MOPAC 4 package [13]. Radical structures

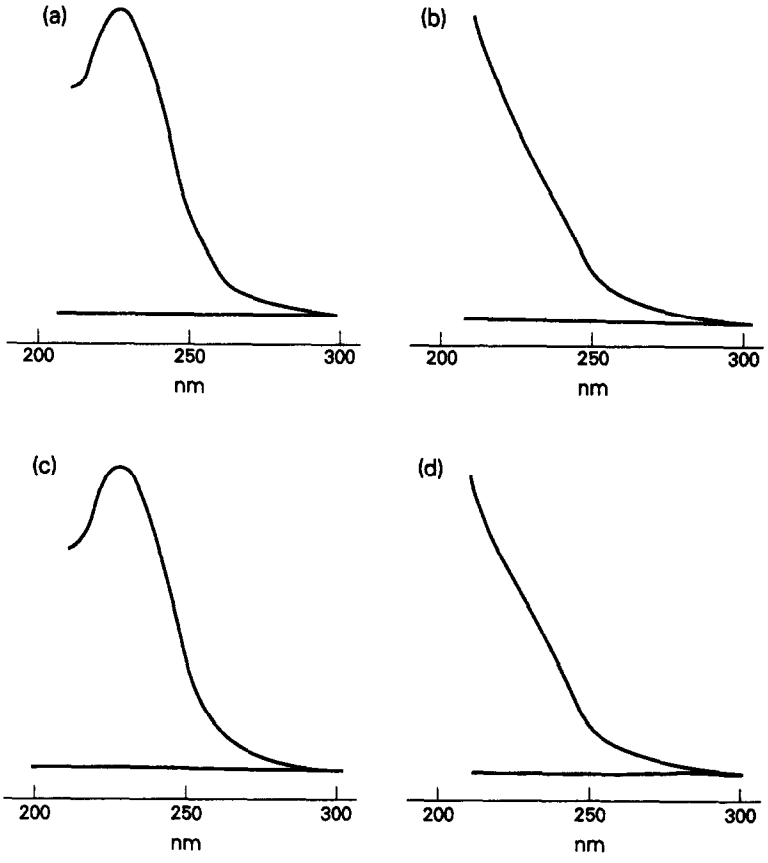

Fig. 3. Diode array UV spectra of (a) *N*-methylbenzamide, (b) *N*-hydroxymethyl-*N*-methylbenzamide, (c) the microsomal metabolite with 6.3 min retention time, (d) the microsomal metabolite with 5.2 min retention time.

were determined using unrestricted Hartree–Fock calculations. All structures were geometry optimized using the Broyden–Fletcher–Goldfarb–Shanno procedure. Computations were performed on a VAX cluster.

RESULTS AND DISCUSSION

The incubation of *N,N*-dimethylbenzamide with rat liver microsomes produces two amide metabolites detectable by HPLC; the minor product has a retention time identical to that of *N*-methylbenzamide (6.3 min), the major product a shorter retention time (5.2 min) consistent with it being more hydrophilic. When aliquots of the reaction mixture are treated with NaOH prior to injection only *N*-methylbenzamide was detected, and its concentration increased markedly (Fig. 2).

Both Ross *et al.* [14] and Hall and Hanzlik [15] have reported previously the formation of a base-labile compound in the microsomal oxidation of *N,N*-dimethylbenzamide which decomposed to *N*-methylbenzamide. Both groups proposed *N*-hydroxymethyl-*N*-methylbenzamide as the identity of the metabolite based on data from GC–MS of a bis(trimethylsilyl)trifluoroacetamide derivatized reaction sample. Unfortunately, attempts to synthesize *N*-hydroxymethyl-*N*-methylbenzamide were unsuccessful [14]. We were keen to establish the identity of this metabolite, so we undertook its synthesis. Despite the fact that *N*-hydroxymethyl-*N*-alkylamides have been reported to be unstable [16] and we ourselves had previously been unable to synthesize such compounds, [17] the synthesis was achieved remarkably simply by mixing *N*-methylbenzamide with a 37% formaldehyde solution at ambient temperature for 24 hr. The yield, as determined by HPLC, was 11% and the product was isolated and purified by semi-preparative HPLC. The product was characterized by ^{1}H and ^{13}C NMR, i.r. and mass spectrometry (see Materials and Methods). The most salient spectroscopic features consistent with the *N*-hydroxymethyl-*N*-methylbenzamide structure are: (i) the N-CH_2O and —OH absorptions at δ_H 4.64 and 6.16 ppm, respectively (these signals were broad but did not reveal the expected coupling, presumably because the proton exchange was too fast even in dimethyl sulphoxide solvent); (ii) two N-CH_2O absorptions, at δ_C 76.8 and 72.9 ppm, corresponding to the *E*- and *Z*-diastereomers, respectively; (iii) two N-CH_3 absorptions at δ_C 38.9 and 34.8 ppm, corresponding to the *Z*- and *E*-diastereomers, respectively; and (iv) the presence of peaks at $m/z = 165$ ($M^{+\cdot}$) and 134

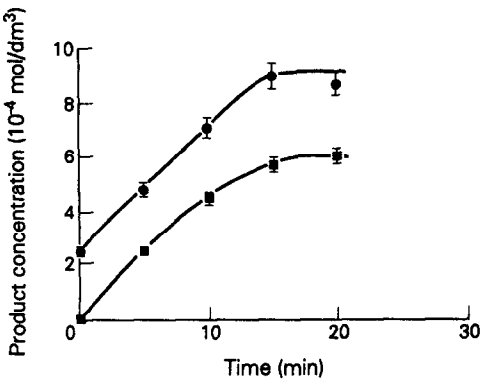

Fig. 4. Time course for the production of *N*-methylbenzamide (■) and formaldehyde (●) during the microsomal metabolism of **1a**.

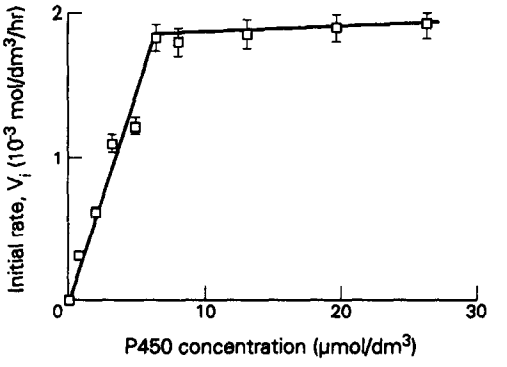

Fig. 5. Plot of initial rate, V_i, versus the microsomal P450 content.

($M^{+\cdot} - CH_2OH$) in the mass spectrum. The presence of *E*- and *Z*-diastereomers is consistent with the work of Gate *et al.* [16], and our assignment of the absorptions in the ^{13}C NMR spectrum to the two diastereomers follows their analysis. The relative intensities of the two N—CH_2—O and two N—CH_3 absorptions indicates that the equilibrium mixture contains the *E*- and *Z*-diastereomers in a ratio of 78:22.

The synthetic sample of *N*-hydroxymethyl-*N*-methylbenzamide had HPLC characteristics identical to the unknown microsomal metabolite, namely retention time and UV spectrum (as obtained by diode array detection) (Fig. 3). However, to identify further the unknown metabolite, it was isolated by semi-preparative HPLC and identified as *N*-hydroxymethyl-*N*-methylbenzamide by mass spectrometry. Significantly, *N*-hydroxymethyl-*N*-methylformamide has been identified as the major urinary metabolite of *N,N*-dimethylformamide using ^1H NMR spectroscopy [18]. This same pattern of metabolism occurs for all the *N,N*-dimethylbenzamides studied, and results in the formation of unstable *N*-hydroxymethyl-*N*-methylbenzamides which subsequently decompose to the corresponding *N*-methylbenzamides and formaldehyde:

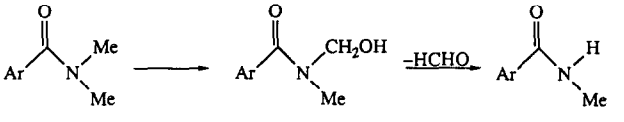

1 2 3

Since *N*-hydroxymethyl-*N*-methylbenzamides decompose in alkaline medium to *N*-methylbenzamides and formaldehyde, the rate of the microsomal demethylation can be obtained by first decomposing the *N*-hydroxymethyl-*N*-methylbenzamides with NaOH, followed by quantification of the *N*-methylbenzamides or formaldehyde formed.

Microsomal oxidations of **1**; **a–f** were monitored by following both the release of HCHO and the formation of the *N*-methylbenzamide **3** (Fig. 4). Interestingly, the time curves for the appearance of these two products were parallel but the release of formaldehyde was always higher than the formation of the *N*-methylbenzamide. This is probably due to the basal metabolism of microsomes since HCHO was identified in incubations where the benzamides were not present. The rate of formation of formaldehyde and *N*-methylbenzamide was found to be linear up to *ca.* 15 min. We chose, therefore, to measure the rate of demethylation using the formation of *N*-methylbenzamide during the initial 12 min period. Independent experiments showed that *N*-methylbenzamide was not significantly metabolized on the time scale of these experiments.

The initial rate varies linearly with the quantity of liver microsomes used in each incubation up to cytochrome P450 concentrations of *ca.* 7 μmol/dm^3, at which point saturation is reached (Fig. 5). This is almost certainly because of the limited amount of NADPH available, and an increase in the amount of NADPH brings about a further increase in the rate (data not shown). Throughout the remainder of this work a cytochrome P450 concentration of 5 μmol/dm^3 was used.

A plot of the initial rate, V_i, versus [substrate] for **1a** is shown in Fig. 6. Interpolation of the data in Fig. 6 using a non-linear least squares method gives rise to the V_{max} and V_{max}/K_m values in Table 1. Corresponding values obtained from similar plots for compounds **1**; **b–f** are also included in Table 1. A comparison of the data for **1a** and **b** shows that there is no significant *inter*molecular kinetic deuterium isotope effect in V_{max} (0.9) or V_{max}/K_m (1.4). Compound **1c** has, of course, very similar global kinetic constants to compounds **1a** and **b**. Thus, the contribution of the C—H bond breaking step to the rate of dealkylation is suppressed by a high commitment to catalysis; that is, the rate of the C—H bond breaking step is large with respect to the rate of substrate release.

That there is a significant isotope effect in the

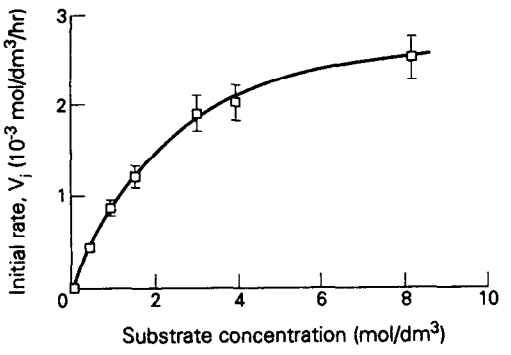

Fig. 6. Plot of initial rate, V_i, versus substrate concentration for **1a**.

C—H(D) bond breaking process can be seen from the *intra*molecular isotope effect, which is determined via the amount of *N*-methylbenzamide versus *N*-trideuteriomethylbenzamide formed in the dealkylation of **1c**. The intramolecular isotope effect so obtained is 6.0 (±0.3). This result is in good agreement with those of Hall and Hanzlik [15], who reported isotope effects in the range 4–7 for the microsomal N-demethylation of tertiary amides. Thus, there is a relatively large intrinsic isotope effect for this reaction.

The data in Table 1 demonstrate that the substituent in the benzene ring clearly has little effect on either V_{max} or V_{max}/K_m. [We observed that *N*,*N*-dimethyl-4-nitrobenzamide, **1f**, is also competitively metabolized to *N*,*N*-dimethyl-4-aminobenzamide (via reduction of the nitro group), but since the reactions were monitored by the formation of the *N*-methyl-4-nitrobenzamide product the values of V_{max} or V_{max}/K_m in Table 1 correctly represent the rate of demethylation. The relative amounts of these two competing pathways appears to depend on the batch of microsomes used. For the data in Table 1 the main product was *N*-methyl-4-nitrobenzamide. However, we observed *N*,*N*-dimethyl-4-aminobenzamide as the major product with other batches of microsomes. We did not pursue these differences further, though Hall and Hanzlik [15] reported that *N*,*N*-dimethyl-3-amino-5-nitrobenzamide was the only product in the microsomal oxidation of the related compound *N*,*N*-dimethyl-3,5-dinitrobenzamide]. Despite this lack of dependence of the kinetic parameters upon the aromatic substituent, there is a significant dependence of the ionization potentials of the amides upon such substituents (Table 1). In contrast the N-demethylation of *N*,*N*-dimethylanilines shows a clear dependence of both V_{max} and V_{max}/K_m upon the ionization potential of the amine, and this has led to the proposal that a single electron transfer, from the amino nitrogen atom to the haem centre of cytochrome P450, is rate limiting [19–21].

Our results lead us to outline a potential mechanism for the conversion of the *N*,*N*-dimethylbenzamide **1** to the *N*-hydroxymethyl-*N*-methylbenzamide **2**. As for the analogous *N*,*N*-dimethylamines, potential pathways involve single electron transfer to form a radical cation **4** or electron abstraction to form the carbon centred radical **5** (Scheme 1) [22]. The radical cation **4** may lose H^+ to form the radical **5** or H$^\cdot$ to form the iminium ion **6**. Both **5** and **6** are capable of interacting with the appropriate haem hydroxyl complex to form the hydroxymethylbenzamide **2**.

Miwa *et al.* has identified criteria for H^+ or H$^\cdot$ loss; H^+ loss is though to be associated with an intrinsic kinetic deuterium isotope effect, <*ca.* 3.6, whereas H$^\cdot$ loss is thought to be associated with an isotope effect, >7 [22]. We observe an intramolecular isotope effect of 6.0, which is a good approximation to, but less than, the intrinsic isotope effect for a reaction [23], from which we deduce that hydrogen is lost as H$^\cdot$. Whether this H$^\cdot$ is lost from the substrate **1** or from the radical cation **4** can be ascertained from the effect of the aromatic substituent. For the analogous dimethylanilines, direct hydrogen atom abstraction from substrate is associated with a Hammett ρ value of *ca.* 0, whereas formation of a radical cation is associated with a Hammett ρ value between −0.6 and −1.0 [19–21]. Our data reveal that there is little correlation between log V_{max} or log V_{max}/K_m and either the Hammett σ substituent constant or the ionization potential calculated by the semi-empirical AM1 procedure. Thus, the kinetic constants are largely independent of the ability of the benzamide to lose an electron and implies the H$^\cdot$ abstraction takes place from the substrate **1** rather than the radical cation **4**. Biomimetic demethylation of dimethylbenzamides using tetraphenylporphyrinatoiron (III) chloride *tert*-butylhydroperoxide yields similar results [8]. For these reasons, we exclude the radical cation **4** as an intermediate in the microsomal reaction and conclude that the metabolism of dimethylbenzamides involves for-

Table 1. Kinetic parameters and ionization for the metabolism of *N*,*N*-dimethylbenzamides by rat liver microsomes at 37° and pH 7.4

Substrate	$10^3 V_{max}$ (mol/dm^3/hr)	$10^3 K_m$ (mol/dm^3)	V_{max}/K_m (hr)	Ionization potential (eV)
1a	3.31	2.49	1.33	9.55
1b	3.70	3.84	0.97	
1c	2.90	2.30	1.30	
1b	1.64	1.42	1.15	9.26
1e	3.55	2.21	1.60	9.66
1f	2.05	1.85	1.11	10.01

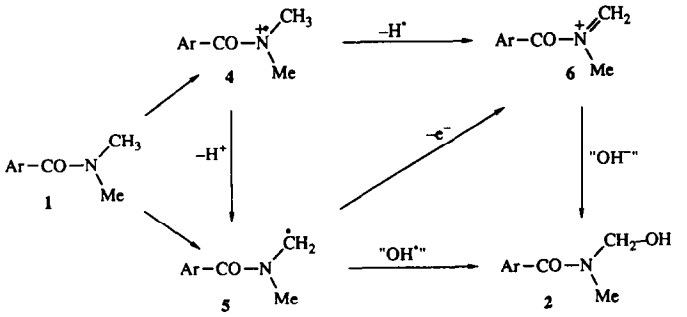

Scheme 1. Pathways for the microsomal oxidation of *N,N*-dimethylbenzamides to *N*-hydroxymethyl-*N*-methylbenzamides.

Table 2. Heats of formation, ΔH_f, for the amides **1**; **a**, **d–f** and the corresponding radicals **5**

	ΔH_f (kJ/mol)			
	1a	**1d**	**1e**	**1f**
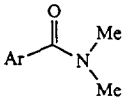	−21.7	−181.5	−50.5	−1.9
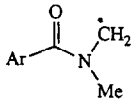	81.1 (102.8)	−78.6 (102.9)	52.6 (103.1)	102.3 (104.2)
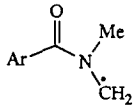	76.5 (98.2)	−83.5 (98)	47.7 (98.2)	97.3 (99.2)

Values in parentheses are the $\Delta\Delta H_f$ values between the radical and the parent amide.

mation of the carbon centred radical **5** via direct hydrogen atom transfer. Our results are unable to identify whether the radical **5** undergoes subsequent electron transfer to form the iminium ion **6**, or whether it is trapped by the haem hydroxyl complex to form the *N*-hydroxymethyl product. However, AM1 self consistent field molecular orbital calculations are able to indicate from which methyl group the hydrogen atom is most likely to be abstracted. The ΔH_f values in Table 2 clearly demonstrate that abstraction of a hydrogen atom from the methyl group *E*- to the carbonyl oxygen atom is favoured by *ca.* 5 kJ/mol over similar hydrogen atom abstraction from the *Z*-methyl group. Significantly, the data in Table 2 indicate that hydrogen atom abstraction from either the *Z*- or the *E*-methyl groups in the dimethylbenzamides is essentially independent of the substituent, as we have observed experimentally. Thus, the data point to a mechanism which involves hydrogen atom abstraction from the *E*-methyl group to form a carbon centred radical **5**.

One important caveat must be made to the above discussion. As described above, we have, in common with other authors, followed the assumption that kinetic deuterium isotope effects <3.6 are associated with H^+ loss and that those ≥7 imply $H^\cdot$ loss. This assumption is now seriously in doubt following the recent work of Dinnocenzo and Banach [24] and Parker and Tilset [25]. Both groups have studied the deprotonation of tertiary amine cation radicals, using bases such as acetate, pyridine and quinuclidine, and have observed isotope effects ranging from 3.6 to 22! The magnitude of deuterium isotope effects on its own therefore appears to be unable to distinguish between the two mechanisms of H loss. Consequently, we are studying currently the microsomal demethylation and dealkylation of a variety of *N*-alkyl-*N*-methylbenzamides and shall report our results in a subsequent paper.

Acknowledgement—We would like to thank JNICT (Portugal) for their financial support to L.C. through the award of grant (number BD/1061.1D).

REFERENCES

1. Guengerich FP, Multiple forms of cytochrome P450, *ISI Atlas Sci Pharmacol* 205–207, 1987.

2. Alexander LS and Goff HM, Chemicals, cancer and cytochrome P450. *J Chem Ed* **59**: 179–182, 1982.
3. Foster AB, Jarman M, Stevens JD, Thomas P and Westwood JH, Isotope effects in *O*- and *N*-demethylations mediated by rat liver microsomes: an application of direct insertion electron impact mass spectrometry. *Chem Biol Interact* **9**: 327–340, 1974.
4. Iley J and Ruecroft G, Mechanism of the Microsomal demethylation of 1-aryl-3,3-dimethyltriazenes. *Biochem Pharmacol* **40**: 2123–2128, 1990.
5. *Martindale the Extra Pharmacopoeia*, 29th Edn, (Ed. Reynolds JEF), p. 1446. The Pharmaceutical Press, London, 1989.
6. Robbins PJ and Cherniak MG, Review of the biodistribution and toxicity of the insect repellent *N,N*-diethyl-*m*-toluamide (DEET). *J Toxicol Environ Health* **18**: 503–525, 1986.
7. Mráz J, Cross JH, Gescher A, Threadgill MD and Flek J, Differences between rodents and humans in the metabolic toxification of *N,N*-dimethylformamide. *Toxicol Appl Pharmacol* **98**: 507–516, 1989.
8. Iley J, Costantino L, Norberto F and Rosa E, Oxidation of the methyl groups of *N,N*-dimethylbenzamides by a cytochrome P-450 mono-oxygenase model system. *Tetrahedron Lett* **31**: 4921–4922, 1990.
9. Furniss BS, Hannaford AJ, Rogers V, Smith PWG and Tatchell AR, *Vogel's Textbook of Practical Organic Chemistry*, 4th Edn, pp. 682–683. Longman, Harlow, 1978.
10. Lowry OH, Rosebrough NJ, Farr AL and Randall RJ, Protein measurement with the Folin phenol reagent. *J Biol Chem* **193**: 265–275, 1951.
11. Omura T and Sato R, The carbon monoxide binding pigment of liver microsomes. I. Evidence for its hemoprotein nature. *J Biol Chem* **239**: 2370–2378, 1964.
12. Nash T, The colorimetric estimation of formaldehyde by means of the Hantzsch reaction. *J Biol Chem* **55**: 416, 1953.
13. MOPAC 4.0, Quantum chemistry programme exchange, QPCE program no. 455, Indiana University.
14. Ross D, Farmer PB, Gescher A, Hickman JA and Threadgill MD, The formation and metabolism of *N*-hydroxymethyl compounds. III. The metabolic conversion of *N*-methyl and *N,N*-dimethylbenzamides to *N*-hydroxymethyl compounds. *Biochem Pharmacol* **32**: 1773–1781, 1983.
15. Hall LR and Hanzlik PR, Kinetic deuterium isotope effects on the *N*-demethylation of tertiary amides by cytochrome P-450. *J Biol Chem* **265**: 12349–12355, 1990.
16. Gate EN, Hooper DL, Stevens MFG, Threadgill MD and Vaughan K, ^{1}H and ^{13}C NMR spectra of the rotational isomers of *N*-hydroxymethylamides and derivatives. *Magn Res Chem* **23**: 78–82, 1985.
17. Iley J, Moreira R and Rosa E, Acyloxymethyl as a drug protecting group. Kinetics and mechanism of the hydrolysis of *N*-acyloxymethylbenzamides. *J Chem Soc Perkin Trans* **2**: 563–570, 1991.
18. Kestell P, Gill MH, Threadgill MD, Gescher A, Howarth OW and Curzon EH, Identification by proton n.m.r. of *N*-(hydroxymethyl)-*N*-methylformamide as a major urinary metabolite of *N,N*-dimethylformamide in mice. *Life Sci* **38**: 719–724, 1986.
19. Burka LT, Guengerich FP, Willard RJ and MacDonald TL, Mechanism of cytochrome P-450 catalysis. Mechanism of *N*-dealkylation and amine oxide deoxygenation. *J Am Chem Soc* **107**: 2549–2551, 1985.
20. Galliani G, Rindone B, Dagnino G and Salmona M, Structure reactivity relationships in the microsomal oxidation of tertiary amines. *Eur J Drug Metab Pharmacokinet* **9**: 289–293, 1984.
21. Galliani G, Nali M, Rindone B, Tollari S, Rochetti M and Salmona M, The rate of *N*-demethylation of *N,N*-dimethylanilines and *N*-methylanilines is related to their first ionisation potential, their lipophilicity and to a steric bulk factor. *Xenobiotica* **16**: 511–517, 1986.
22. Miwa GT, Walsh JS, Kedderis GL and Hollenberg PF, The use of intramolecular isotope effects to distinguish between deprotonation and hydrogen atom abstraction mechanisms in cytochrome P450 and peroxidase-catalysed *N*-demethylation reactions. *J Biol Chem* **258**: 14445–14449, 1983.
23. Miwa GT, Garland WA, Hodston BJ, Lu AYH and Northrop DB, Kinetic isotope effects in cytochrome P-450 catalysed oxidation reactions. *J Biol Chem* **255**: 6049–6054, 1980.
24. Dinnocenzo JP and Banach TE, Deprotonation of tertiary amine cation radicals. A direct experimental approach. *J Am Chem Soc* **111**: 8646–8653, 1989.
25. Parker VD and Tilset M, Facile proton transfer reactions of *N,N*-dimethylaniline cation radicals. *J Am Chem Soc* **113**: 8778–8781, 1991.